

Worcester Polytechnic Institute Digital WPI

Major Qualifying Projects (All Years)

Major Qualifying Projects

April 2013

Macroscopic Modeling of Microwave-enabled Solution-processable Graphene

Chuqiao Yang

Worcester Polytechnic Institute

Follow this and additional works at: <https://digitalcommons.wpi.edu/mqp-all>

Repository Citation

Yang, C. (2013). *Macroscopic Modeling of Microwave-enabled Solution-processable Graphene*. Retrieved from <https://digitalcommons.wpi.edu/mqp-all/1328>

This Unrestricted is brought to you for free and open access by the Major Qualifying Projects at Digital WPI. It has been accepted for inclusion in Major Qualifying Projects (All Years) by an authorized administrator of Digital WPI. For more information, please contact digitalwpi@wpi.edu.

Project Number: VVY-1202

**MACROSCOPIC MODELING OF MICROWAVE-ENABLED PRODUCTION OF
SOLUTION-PROCESSABLE GRAPHENE**

A Major Qualifying Project Report:

submitted to the faculty

of the

WORCESTER POLYTECHNIC INSTITUTE

in partial fulfillment of the requirements for the

Degree of Bachelor of Science

by

Chuqiao Yang

April 25, 2013

Advised by:

Professor Vadim Yakovlev

Professor Alex Zozulya

Abstract

Numerous microwave-assisted chemical reactions offer such benefits as shorter reaction times, higher product yields, and enhanced selectivity. In particular, a new promising technique for microwave-enabled production of graphene sheets demonstrates an unprecedentedly short production time, better quality product, and the potential for low-cost mass production. However, in the traditional framework, further development of this technique would require laborious, inefficient and expensive trial-and-error experiments aiming to correlate the input parameters of the microwave reactor and the output characteristics of the product. This MQP contributes to an open-ended research aiming to facilitate the development of this technology of production of graphene up to the level of mass production through dedicated mathematical modeling. We introduce three models:

- (1) predicting 3D temperature field inside solid/high viscosity reactant by solving Maxwell's equations coupled with the heat equation using finite-difference time-domain technique;
- (2) estimating average temperature of well-stirred/low viscosity liquid reactants through a simplified physics-based model (showing excellent correspondence with experimental data); and
- (3) studying the selective heating effect through modeling temperatures of two components of the reactant in the microwave-enabled technology of production of graphene, graphite powder and concentrated H_2SO_4 and HNO_3 .

The models can be used with a variety of carbon nanomaterials and other microwave reactors to generate temperature characteristics and guide microwave-assisted production of other new materials.

Acknowledgement

This work was partially supported by the Office of the WPI Dean of Arts and Sciences. The author is grateful to:

- SAIREM SAS, Neyron, France – for providing *MiniFlow 200SS* system for modeling and experimentation;
- Andrew O. Holmes, WPI ('13) – for cooperation in the development of the coupled model in *QuickWave-3D* and in the experiments with *MiniFlow 200SS*;
- Prof. Huixin He, Mehulkumar Patel, Keerthi Savara, Chemistry Department, Rutgers University, Newark, NJ – for discussion of motivation of this study and the underlying concepts in chemistry;
- Prof. Burt Tilley, Mathematical Sciences, WPI – for discussing the related issues in partial differential equations;
- Prof. Stephan Koehler, Physics, WPI – for discussing issues in physical experimentation;
- Prof. Jose M. Catalá-Civera, Polytechnic University of Valencia, Valencia, Spain – for measuring dielectric properties of reactants.

Contents

Abstract	i
Acknowledgments	ii
List of Figures & Tables	iv
1 Introduction	1
2 Microwave Reactor & Numerical Model	4
3 Simplified Temperature Model	8
3.1 Mathematical Model	-
3.2 Computational Results and Experimental Validation	13
3.3 Discussion	16
4 Model of Selective Heating	18
5 Conclusions	22
Appendix. MATLAB Codes	24
References	29

List of Figures & Tables

Figure 2.1. SAIREM *MiniFlow 200SS* system; general view and a model-generated representation of the interior of its microwave unit

Figure 2.2. Simulated microwave-induced temperature of water heated in *MiniFlow 200SS* (microwave power 100 W)

Figure 2.3. Experimental setup: *MiniFlow 200SS* with a fiber optic sensor inside a glass capillary vertically inserted into the Pyrex vial and a zoom-in view of the vial

Figure 2.4. Evolution of temperature in 15.6 ml sample of water (50 mm height) at different distances h from the bottom of the vial – 16 mm (a) and 28 mm (b); measurement performed every 3 s; simulated characteristics are shown by solid curve; microwave power 100 W, frequency 2.45 GHz

Figure 3.1. Cross-section of a three-media cylindrical element of a microwave reactor

Figure 3.2. Heat flux at the boundaries of all three media

Figure 3.3. Average reflected power in six experiments of microwave heating of water (15.7 g) in *MiniFlow 200SS* by 100 W of incident power

Figure 3.4. Average temperature of a 15.7 g sample of water as function of heating time – model (18)-(19) and measurement

Figure 3.5. Computed time evolution of average temperatures of the 15.7 g ethanol and methanol samples in *MiniFlow 200SS*, for absorbed power 100 W and 90 W

Figure 4.1. Setup of model considering graphite powder and acids separately

Figure 4.2. Simulation results for temperature of graphite and the acids as a function of distance from the center of the graphite domain at different time instances t

Figure 4.3. Simulated temperature distributions (normalized to the maximum temperature of the process) in the vertical planes through the center of the reactor

Table 3.1. Geometrical Parameters and Masses of the *MiniFlow 200SS* Reactor.

Table 3.2. Thermal Media Parameters Used in Simulation.

1 Introduction

Microwave-assisted chemistry is a rapidly growing discipline utilizing microwaves as a means of enhancing and accelerating chemical reactions. Microwave heating is the phenomenon behind such advantages as accelerated reaction rate, higher chemical yield, lower energy use, and some other benefits observed in comparison with conventional heating methods [1, 2]. Currently, there exists a range of dedicated equipment for use in preparative chemistry; however, the development of new reaction routes remains difficult because of a lack of data on the interaction between the reactants and corresponding microwave units [2, 3].

Recently, a promising technique has been developed for microwave-enabled production of highly conductive solution-processable graphene sheets [4]. On the level of lab experiments, this technique demonstrates an unprecedentedly short production period, capability of producing graphene sheets of much larger size and with fewer defects, and has the potential for low-cost mass production. However, any upgrade of this microwave-assisted technique to the industrial level would require, in the framework of the traditional approach, a significant number of trial-and-error experiments aiming to demonstrate some correlation between the input parameters of the microwave reactor and the output characteristics of the product, and such work may be laborious and inefficient.

This MQP was initiated as open-ended research aiming to facilitate the development of an efficient microwave-assisted technology for mass production of solution-processable graphene through the use of suitable macroscopic models. At the starting point of the project, a motivated conceptual decision was made to focus on macroscopic modeling of the process outlined in [4] and characterize the reactants in terms of electromagnetic (EM) and thermal (T) parameters (and thus to exclude the related chemical processes and physical micro-scale phenomena from consideration).

It appears that sufficiently adequate computer models could help clarify certain issues and help further develop the technique [6]. Indeed, modeling of the underlying EM and T processes has already found a well-defined niche in other technologies employing microwave energy, such as food and materials processing, as a useful and instructive tool determining the key characteristics and assisting in design of microwave applicators [5, 7-9]. Moreover, in [9], a modeling-based technique has been proposed to specifically design/scale up energy efficient microwave reactors.

This project makes an attempt to continue the development started in [9] and explore a number of options in macroscopic modeling applicable to the process of microwave-assisted chemistry and, in particular, to the new technique of production of graphene [4]. Our effort is primarily dedicated to mathematical models aiming to predict temperature of the reactant exposed to microwaves.

More specifically, we present here a simple analytical model allowing for determining the average temperature of a liquid reactant well stirred due to the convection effect. We consider a three-media concentric cylindrical structure containing the reactant, a vessel, and a container holding the vessel. The whole structure is presumed to be inside a closed metal cavity (a waveguide or a resonator) and heated by microwaves. This scenario is natural for preparative microwave-assisted chemistry and can be found implemented in some dedicated commercial equipment. The developed model is used in this project to compute time evolution of the average temperature of water in a Pyrex vial inside a Teflon cup; geometrical parameters are taken as in the *MiniFlow 200SS* batch reactor. Modeling results are found to be in an excellent agreement with temperature values measured by a fiber optic sensor. The validated model

is finally used for estimation of temperature evolution of two other substances (ethanol and methanol) heated in the same reactor.

This approach is further advanced in this MQP by constructing a simplified model of microwave heating of graphite powder in the mixture of two acids (H_2SO_4 and HNO_3), i.e., of the reactant in the technique [4]. We have made initial progress toward computationally demonstrating that it is possible to selectively heat graphite powder up to temperatures much higher than that of the acid mixture. Additional input into these studies is made by full-wave 3D FDTD simulation of the temperature field in the graphite-acid mixture (under the assumption that the reactant has no convection). These preliminary results suggest a series of particular steps that would further assist in modeling-based development of the new microwave-enabled technology of production of graphene.

2 Microwave Reactor & Numerical Model

At the first stage of our project, we develop an advanced numerical model capable of simulating EM and T phenomena in the *MiniFlow 200SS* batch reactor (Figure 2.1), a commercially available apparatus for microwave-assisted chemistry that is designed, manufactured and put on the market by SAIREM SAS, Neyron, France. The reactor consists of a cylindrical cavity containing a concentrically positioned cylindrical Teflon cup intended for holding the reactant in a cylindrical Pyrex vial. *MiniFlow 200SS* belongs to a group of innovative highly efficient microwave reactors: it is fed, via a coaxial cable, by a solid-state generator providing a robust control over frequency of excitation (in the range from 2.43 to 2.47 GHz) and magnitude of the signal (from 0 to 200 W). As such, the reactor is an excellent candidate for developing new controllable and reproducible reactions of microwave-assisted chemistry.

The *MiniFlow 200SS* reactor has been precisely reproduced in a 3D parameterized model developed for the full-wave 3D conformal FDTD simulator *QuickWave-3D (QW-3D)* [10]. Components of the reactor and the reactant are represented in the model by their shapes as well as their thermal and dielectric parameters. Input data needed for the model are: density ρ , specific

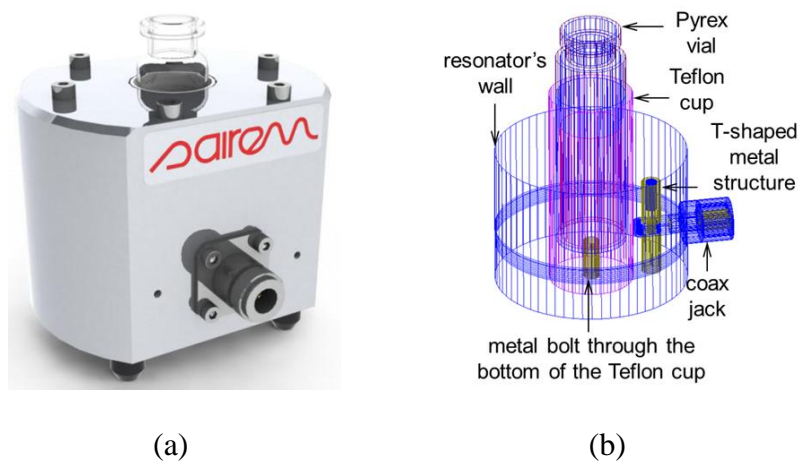


Figure. 2.1. *MiniFlow 200SS* batch reactor from SAIREM SAS: general view (a) and a model-generated representation of the interior of its microwave unit (b).

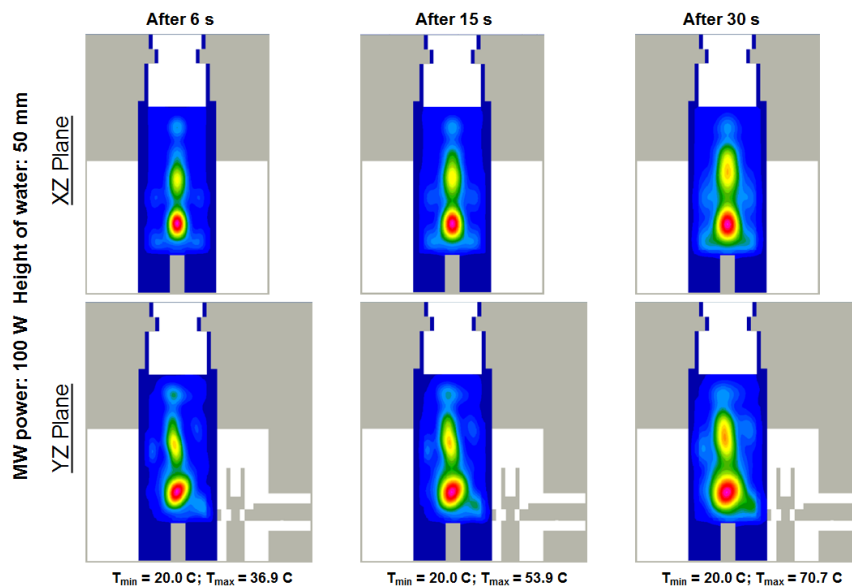


Figure 2.2. Simulated microwave-induced temperature of water heated in *MiniFlow 200SS* (microwave power 100 W)

heat c , thermal conductivity k , and complex permittivity $\varepsilon = \varepsilon' - i\varepsilon''$ (where ε' is dielectric constant and ε'' is the loss factor) of the reactant, a Pyrex vial, and a Teflon holder. The same modeling concept can be used to build multiphysics models of the same capacity for other equipment.

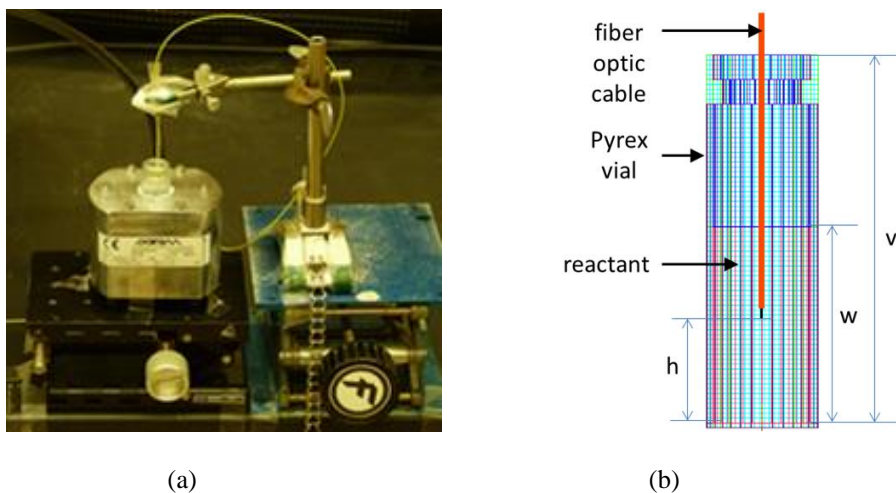


Figure 2.3. Experimental setup: *MiniFlow 200SS* with a fiber optic sensor inside a glass capillary vertically inserted into the Pyrex vial (a) and a zoom-in view of the vial (b).

Temperature fields in the reactant were simulated through solving the coupled Maxwell's equations and the heat equation using the conformal 3D Finite Difference Time Domain (FDTD) technique implemented in *QW-3D* [10]. Figure 2.2 shows an example of temperature patterns for water. The model predicts non-uniform heating with a clearly seen focusing effect in the central lower part of the water sample.

Temperature distribution in water heated in the *MiniFlow 200SS* reactor was also measured using the experimental setup shown in Figure 2.3. Temperature is monitored using a fiber optic sensor that moves (being held inside a glass capillary) along the central axis of the vial and measures temperature dynamically in the course of heating.

While two examples comparing measured and simulated time-temperature characteristics (Figure 2.4) generally confirm the adequacy of the developed model, experimental results revealed that in liquid reactants the actual temperature fields are more uniform than they appear in the model's output. We suggest that this might be explained by the presence of convection flows acting as an effective mechanism of averaging the reactant's temperature.

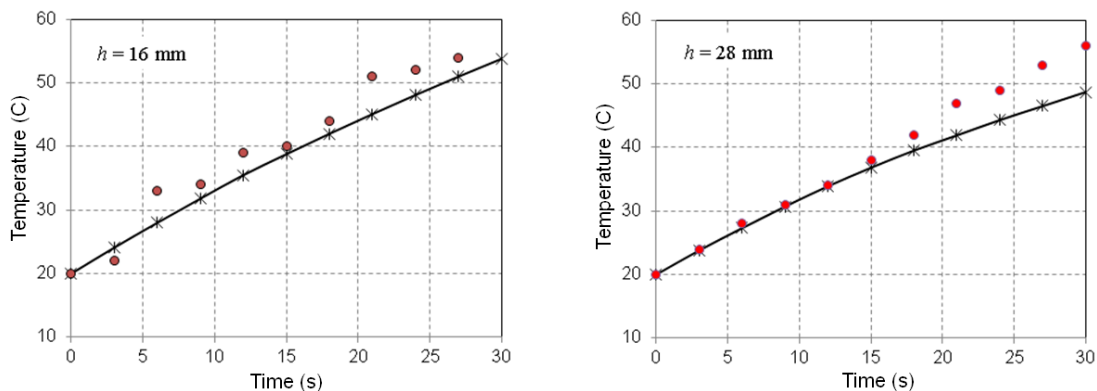


Figure 2.4. Evolution of temperature in 15.6 ml sample of water (50 mm height) at different distances h from the bottom of the vial – 16 mm (a) and 28 mm (b); measurement performed every 3 s (points); simulated characteristics are shown by solid curve; microwave power 100 W, frequency 2.45 GHz; experimental data (dots) and computation (solid curve).

Given the fact that modeling convection flow can be both mathematically complicated and computationally heavy, adding such a model to the already complex and time-consuming EM-T simulation would be impractical. To address convection flows, at the next stage of the project we introduce a simplified physics-based model of microwave heating of arbitrary liquid reactants with strong convection. The last stage of this MQP is focused on the development of original simplified models for temperature of the acid-graphite mixture exposed to microwave radiation.

3 Simplified Temperature Model

3.1 Mathematical Model

In this section, we present a simple model that determines the average temperature of a liquid reactant exposed to microwave heating and well stirred due to the convection effect (or by manual/mechanical stirring). We consider a three-media concentric cylindrical structure (Figure 3.1): Medium 1 is the reactant (a liquid or low viscosity substance), Medium 2 is the material of the vessel (usually glass or Pyrex), and Medium 3 represents a container (made of Teflon or another low loss dielectric) holding the vessel. The whole structure is presumed to be inside a closed metal cavity (a waveguide or a resonator) and heated by microwaves. This scenario is natural for preparative microwave-assisted chemistry and can be found implemented in some dedicated commercial equipment (e.g., in *MiniFlow 200SS*).

The heat transfer problem is formulated for the concentric scenario in Figure 3.1 under the following assumptions:

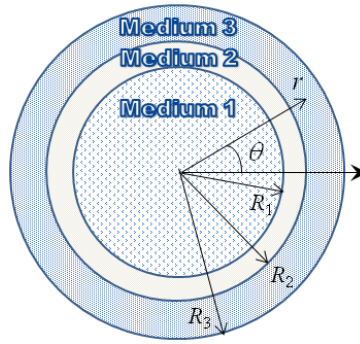


Figure 3.1. Cross-section of a three-media cylindrical element of a microwave reactor.

- Absorbed power per volume is uniform due to strong convection flow.
- Compared to Medium 1 (the reactant) and Medium 3 (e.g., Teflon), Medium 2 (e.g., Pyrex or glass) is usually a material of lower specific heat and smaller mass, so heat absorbed by Medium 2 is negligible.
- Media 2 and 3 do not absorb microwave power.

As an element of a microwave reactor, the concentric structure in Figure 3.1 is confined inside of a metal cavity and surrounded by air. We therefore consider all outer surfaces of this structure (side walls, top, and bottom) to be thermally insulated.

A typical general model of the microwave heating process is based on solving an EM-T coupled problem (i.e., Maxwell's equations coupled with the heat transfer equation, assuming appropriate boundary and initial conditions) and requires the use of advanced numerical techniques and substantial computational resources [6, 7, 9]. In the EM part of the problem, the absorbed microwave power per unit volume is proportional to the squared magnitude of the electric field, which can vary significantly from point to point. However, here we consider substances with strong convection flows that, as seen in the related experiments outlined in Section 2, stir the reactants and homogenize temperature distributions. We thus deduce that the same effect could be produced, in the absence of convection, by a uniform electric

field. Assuming perfect convection, we consider the electric field, as well as the power absorbed by the volume of Medium 1, to be uniform.

Relating the EM problem to the T problem, we consider two heat transfer equations in polar coordinates with the origin in the center of the structure:

$$\begin{aligned} \text{Medium 1: } \frac{\partial u_1}{\partial t} &= \alpha_1 \nabla^2 u_1 + q, \\ \text{Medium 3: } \frac{\partial u_3}{\partial t} &= \alpha_3 \nabla^2 u_3, \end{aligned} \quad (1)$$

where $u_{1,3} = u_{1,3}(r, t)$ denote temperatures, $\alpha_{1,3}$ are thermal diffusivities of Medium 1 and 3, respectively, $q = P_a/c_1 m_1$ is the heat source term due to microwave absorption, where m_1 and c_1 are the mass and specific heat of Medium 1, and P_a is microwave power absorbed by Medium 1.

Aiming to determine the average temperature of the reactant, in the following derivation we reduce the problem to a 1D scenario in which temperature changes only in the r -direction. By expanding in (1) the Laplacian in polar coordinates, we obtain the governing equations:

$$\text{Medium 1: } \frac{\partial u_1}{\partial t} = \alpha_1 \left[\frac{1}{r} \frac{\partial u_1}{\partial r} + \frac{\partial^2 u_1}{\partial r^2} \right] + q, \quad (2)$$

$$\text{Medium 3: } \frac{\partial u_3}{\partial t} = \alpha_3 \left[\frac{1}{r} \frac{\partial u_3}{\partial r} + \frac{\partial^2 u_3}{\partial r^2} \right]. \quad (3)$$

The thermal insulation on the outer surface of Medium 3 is given by the boundary condition:

$$\frac{\partial u_3(R_3, t)}{\partial r} = 0. \quad (4)$$

Also, because of symmetry of the problem around $r = 0$, we assume a zero temperature gradient at the center of Medium 1, i.e.:

$$\frac{\partial u_1(0, t)}{\partial r} = 0. \quad (5)$$

To introduce average temperatures of Media 1 and 3, we integrate both sides of (2) over the portion of the domain occupied by Medium 1. Satisfying the boundary condition (5), we obtain:

$$A_1 \frac{\partial \bar{u}_1}{\partial t} = \alpha_1 \left\{ \int_0^{R_1} \left[\frac{1}{r} \frac{\partial u_1}{\partial r} + \frac{\partial^2 u_1}{\partial r^2} \right] r dr \int_0^{2\pi} d\theta \right\} + A_1 q = 2\pi \alpha_1 R_1 \frac{\partial u_1}{\partial r}(R_1, t) + A_1 q, \quad (6)$$

where $A_1 = 2\pi R_1^2$, and \bar{u}_1 is the average temperature of Medium 1. Then (6) can be re-written as

$$\frac{\partial \bar{u}_1}{\partial t} = D_1 \frac{\partial u_1}{\partial r}(R_1, t) + q, \quad (7)$$

where

$$D_1 = \frac{2\alpha_1}{R_1}. \quad (8)$$

Similarly, we integrate both sides of (3) over the domain and, assuming the boundary condition (4) is satisfied, obtain:

$$A_3 \frac{\partial \bar{u}_3}{\partial t} = \alpha_3 \left\{ \int_{R_2}^{R_3} \left[\frac{1}{r} \frac{\partial u_3}{\partial r} + \frac{\partial^2 u_3}{\partial r^2} \right] r dr \int_0^{2\pi} d\theta \right\} = 2\pi \alpha_3 \left[R_3 \frac{\partial u_3}{\partial r}(R_3, t) - R_2 \frac{\partial u_3}{\partial r}(R_2, t) \right], \quad (9)$$

where $A_3 = \pi(R_3^2 - R_2^2)$ is the area of the domain, and \bar{u}_3 is the average temperature of Medium 3. We then reduce equation (9) to

$$\frac{\partial \bar{u}_3}{\partial t} = -D_3 \frac{\partial u_3}{\partial r}(R_2, t), \quad (10)$$

where

$$D_3 = \frac{2\alpha_3 R_2}{2(R_3 - R_2)R_2 + (R_3 - R_2)^2}. \quad (11)$$

By Fourier's law of conduction, the heat flux (as shown in Figure 3.2) exiting Medium 1 is:

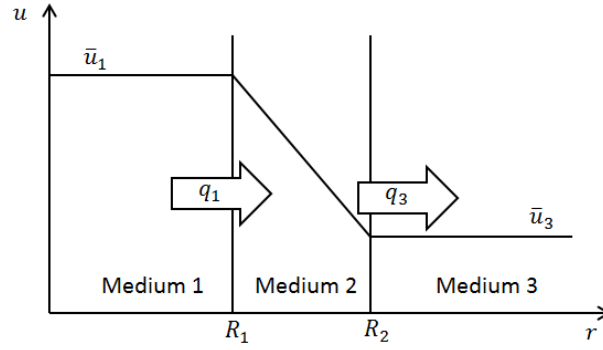


Figure 3.2. Temperature in all three media and the heat flux on their boundaries.

$$q_1 = k_1 \frac{\partial u_1}{\partial r} (R_1, t), \quad (12)$$

where k_1 is thermal conductivity of Medium 1. Similarly, the heat flux entering Medium 3 is:

$$q_3 = k_3 \frac{\partial u_3}{\partial r} (R_2, t), \quad (13)$$

where k_3 is thermal conductivity of Medium 3. The heat flux through Medium 2 could be calculated similarly, but since the thickness of Medium 2 is small, the gradient through it is instead taken to be the difference of temperatures across Medium 2 divided by its thickness (as illustrated in Figure 3.2). The heat flux through Medium 2 is thus expressed as

$$q_2 = \frac{k_2 [\bar{u}_1(R_1, t) - \bar{u}_3(R_2, t)]}{R_2 - R_1}, \quad (14)$$

where k_2 is the thermal conductivity of Medium 2. Because of energy conservation, the heat flux is conserved, i.e.:

$$q_1 = q_2 = q_3. \quad (15)$$

Combining (12) through (15), we find the temperature gradients at R_1 and R_2 in relation to the average temperatures in Media 1 and 3 to be:

$$\frac{\partial u_1}{\partial r}(R_1, t) = \frac{\bar{u}_3 - \bar{u}_1 k_2}{R_2 - R_1 k_1}, \quad (16)$$

$$\frac{\partial u_2}{\partial r}(R_2, t) = \frac{\bar{u}_3 - \bar{u}_1 k_2}{R_2 - R_1 k_3}. \quad (17)$$

Substituting (7) and (10) into (16) and (17), we obtain the following system of differential equations, which can be solved for \bar{u}_1 and \bar{u}_3 :

$$\frac{\partial \bar{u}_1}{\partial t} = -\frac{D_1 k_2}{(R_2 - R_1) k_1} \bar{u}_1 + \frac{D_1 k_2}{(R_2 - R_1) k_1} \bar{u}_3 + \frac{P_a}{c_1 m_1} \quad (18)$$

$$\frac{\partial \bar{u}_3}{\partial t} = \frac{D_3 k_2}{(R_2 - R_1) k_3} \bar{u}_1 - \frac{D_3 k_2}{(R_2 - R_1) k_3} \bar{u}_3. \quad (19)$$

To summarize, the input data needed to solve (18) and (19) are: microwave power absorbed by Medium 1, material parameter of Media 1 and 3 (density, mass, specific heat, and thermal conductivity), and radii of all three cylinders. In the absence of data on thermal diffusivities for (8) and (11), the values of $D_{1,3}$ could be determined through the densities of the respective media as $\alpha_{1,3} = k_{1,3}/(\rho_{1,3} c_{1,3})$.

3.2 Computational Results and Experimental Validation

A computer code solving the system (18)-(19) has been implemented as a MATLAB script using the function `ode45` (see Appendix A). Geometrical and material parameters were taken to replicate the batch reactor of the *MiniFlow 200SS* system; these parameters are presented in Tables 3.1 and 3.2.

Similar to Section 2, experimental validation of the model was made with 15.7 g of water in a cylindrical 30 mm high Pyrex vial. A series of six experiments, each heating this sample up to 80 C by 100 W of incident microwave power at 2.45 GHz, was performed. The values of power and frequency were strictly maintained by the control system of a solid state generator in the *MiniFlow 200SS* system. A fiber optic sensor was used to measure temperature at six different points along the central axis of the vial.

Table 3.1. Geometrical Parameters and Masses of the *MiniFlow 200SS* Reactor

R_1 (mm)	R_2 (mm)	R_3 (mm)	Mass of Pyrex walls (g)	Mass of Teflon walls (g)
10	12	14.3	2	26.3

Table 3.2. Thermal Media Parameters Used in Simulation

	Density (g/m^3)	Specific heat ($\text{J}/(\text{gK})$)	Thermal conductivity ($\text{W}/(\text{mK})$)
Medium 1: water	1.00×10^6 [11]	4.2 [11]	0.6 [11]
Medium 1: ethanol	7.89×10^5 [11]	2.35 [12]	0.167 [11]
Medium 1: methanol	7.93×10^5 [11]	2.53 [11]	0.202 [11]
Medium 2: Pyrex	–	0.75 [12]	1.0 [11]
Medium 3: Teflon	2.20×10^6 [11]	1.45 [13]	0.25 [13]

The absorbed power P_a , an input parameter of the model (18)-(19), was calculated from the reflected power recorded for each heating experiment every 3 seconds; the averaged time characteristic of the reflected power is shown in Figure 3.3.

Figure 3.4 shows the average temperature of Medium 1 (water) obtained from the simulations and measurements. Computational and experimental results are in excellent agreement. This confirms our hypothesis that the convection flows make a significant impact on the microwave-induced temperature fields in liquid reactants. The developed model is therefore directly applicable to any other low viscosity substances (whose mass, density, specific heat, and thermal conductivity are known) heated in other microwave systems featuring a similar cylindrical concentric element as in Figure 3.1.

Figure 3.5 shows the results of application of the model to two other common chemical substances (ethanol and methanol, whose thermal properties are also collected in Table 3.2) in comparison with water. The dimensions of the scenario are again taken as in *MiniFlow 200SS* (Table 3.1).

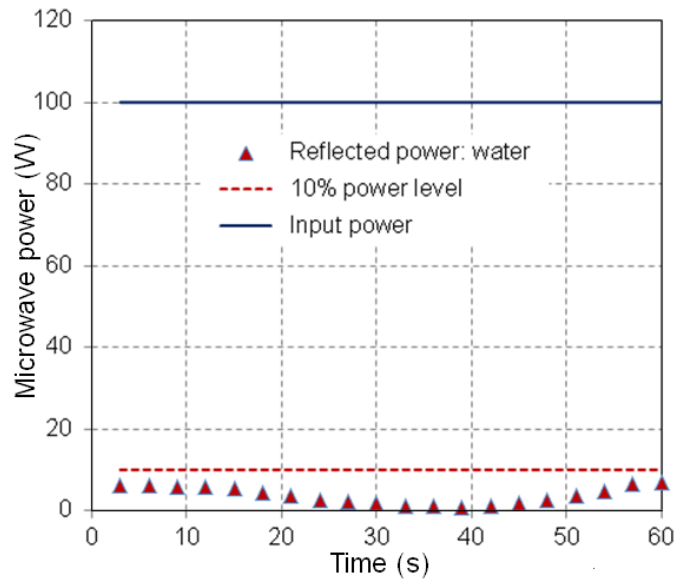


Figure 3.3. Average reflected power in six experiments of microwave heating of water (15.7 g) in *MiniFlow 200SS* by 100 W of incident power.

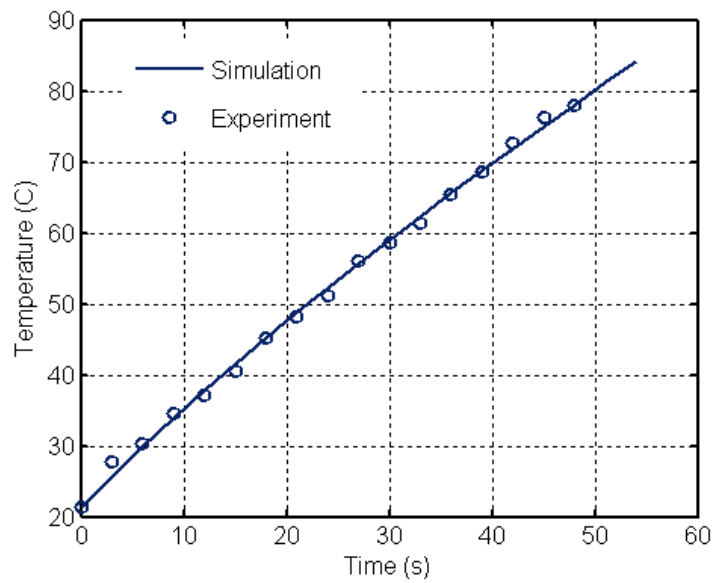


Figure 3.4. Average temperature of a 15.7 g sample of water as function of heating time – model (18)-(19) and measurement.

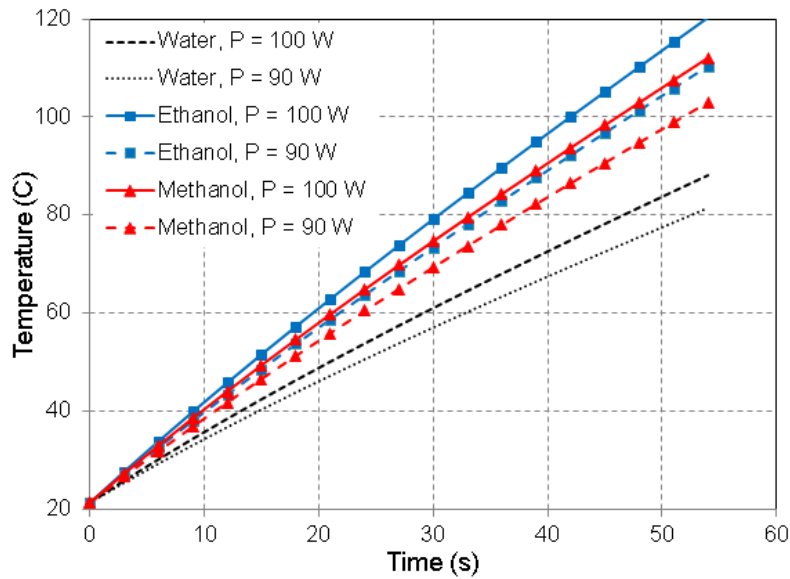


Figure 3.5. Computed time evolution of average temperatures of the 15.7 g ethanol and methanol samples in *MiniFlow 200SS*, for absorbed power 100W and 90W

3.3 Discussion

When solving the heat transfer problem (2)-(5), we employ the approach of integrating the heat equation over its domain rather than analytically solving for temperature distribution, because of our interest in the average temperatures rather than the temperature fields themselves.

In Figure 3.5, we present the upper and lower bounds of the time-temperature characteristics corresponding to zero- and 10% loss of microwave power. These curves were calculated for the particular levels $P_a = 100 \text{ W}$ and $P_a = 90 \text{ W}$ of absorbed (rather than incident) microwave power. As such, Figure 3.5 shows the difference in heating of the considered substances due to their thermal properties rather than their loss factors (which are higher and lower, respectively, for ethanol and methanol compared to that of water [14]), and this calculation is based on the prescribed level of P_a . However, if experimental data on the absorbed power (similar to the one in Figure 3.3) is available prior to calculation with (18)-(19), the

model may be capable of generating a precise time-temperature characteristic of the process (similar to the curve in Figure 3.4).

This consideration suggests that knowledge of reflected (and thus absorbed) power of the microwave-assisted chemical reaction may make the proposed simple model an efficient and accurate computational tool determining average temperature of substances with strong convection. If corresponding equipment and the reactants are not accessible for experimentation, the required characteristics could be produced with the use of appropriate general-purpose electromagnetic modeling software (e.g., *QuickWave-3D* [10]).

4 Model of Selective Heating

After obtaining an operational model for the average temperature of a liquid reactant, we focus on a specific reaction resulting in production of graphene. In a series of experiments [4], graphite powder mixed in concentrated H_2SO_4 and HNO_3 was found to be heated by microwaves more intensively than the acids [15]. The temperature of graphite powder was estimated to be up to 500-1,000°C, while the temperature of the acids was only about 100°C [15].

Aiming to mimic the effect of selective heating of graphite powder in a model, we upgrade the approach described in Section 3 by considering the powder and the acids separately. We assume that graphite powder is sparsely and uniformly placed in the volume of acids, as illustrated in Figure 4.1. The governing equations can then be written down as inhomogeneous heat equations:

$$\text{For graphite: } T_t^{(1)} = \alpha_1 \nabla^2 T^{(1)} + \Phi_1, \quad (20)$$

$$\text{For acids: } T_t^{(2)} = \alpha_2 \nabla^2 T^{(2)} + \Phi_2; \quad (21)$$

with the boundary condition between graphite and acids being a perfect thermal contact, and temperature bounded at infinity:

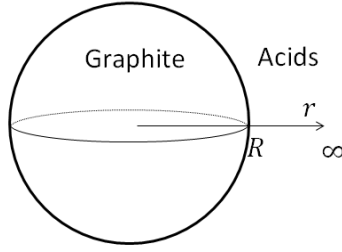


Figure 4.1. Domain of the model considering graphite powder and the acids separately.

$$\text{at } r = R, T^{(1)} = T^{(2)} \text{ and } k_1 T_r^{(1)} = k_2 T_r^{(2)}; \quad (22)$$

$$\text{at } r = \infty, T_r^{(2)} = 0. \quad (23)$$

Since an analytical solution of the system (20) and (21) with the boundary condition (22) and (23) can be very complicated, as a preliminary testing, we solve them numerically in 1D Cartesian setting using a finite difference method with implicit differentiation; corresponding MATLAB code is included in Appendix B. In this solution, we assumed that the EM field inside the mixture of graphite and the acids is uniform. Then the power absorbed by a substance is directly proportional to the volume and the loss factor of the substance. In the absence of data on complex permittivity of H_2SO_4 and NHO_3 , we assume that graphite powder is immersed in water, not in the acids, and use in computation T and EM properties of water.

As it appears in computational results produced from this approach and shown in Figure 4.2, graphite powder is heated to a much higher temperature than water; this seems to be consistent with prior experimentation [15].

In the reaction producing graphene sheets, the chemistry occurs on the surface of graphite particles [4], so the increased temperature of the graphite powder would directly accelerate the reaction. Thus, the selective heating effect may be a possible explanation for the remarkably accelerated reaction rate in the technique [4].

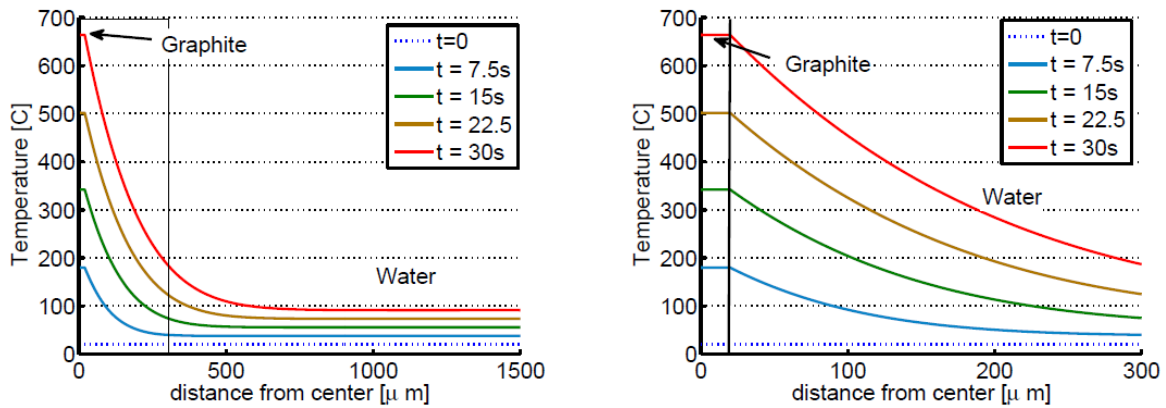


Figure 4.2. Simulation results for temperature of graphite and the acids as a function of distance from the center of the graphite domain at different time instances t – at the 0-1,500 μm scale (a) and at the 0-300 μm scale (b).

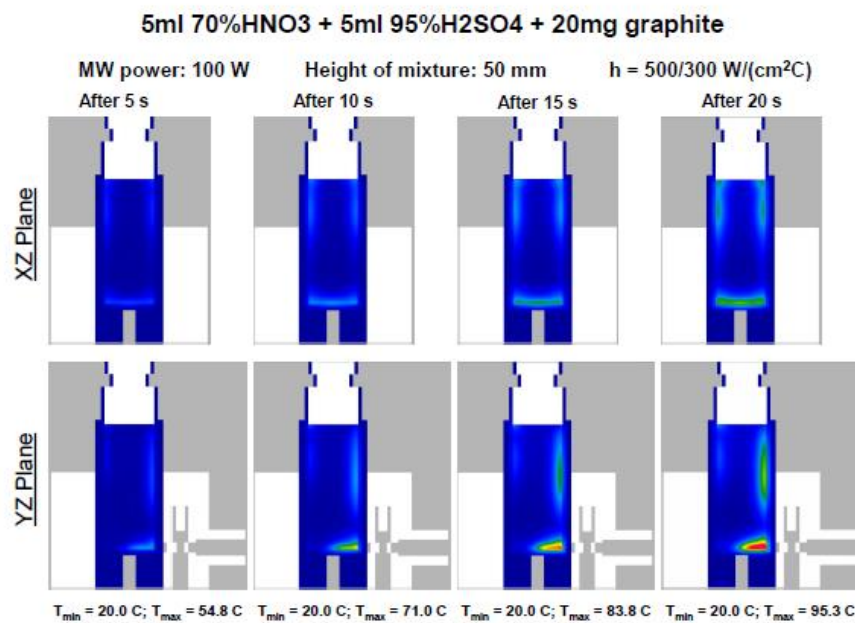


Figure 4.3. Simulated temperature distributions (normalized to the maximum temperature of the process) in the vertical planes through the center of the reactor.

Along with the above numerical solution of the problem (20)-(23), we used the developed QW-3D model of the batch reactor *MiniFlow 200SS* to simulate distribution of the temperature field in the acid-

graphite mixture. Simulations were performed using data on complex permittivity of the mixture (5 ml 70% HNO₃ + 5 ml 95% H₂SO₄ + 20 mg graphite powder) obtained experimentally in [16]. The value of complex permittivity of the mixture at room temperature and at 2.45 GHz was found to be $\epsilon = 26.7 - i99.0$.

In our computational results, shown in Figure 4.3, the temperature is found to be sharply increased in the thin layer of the reactant near its surface, especially in the lower corner adjacent to the excitation element of the reactor. This is consistent with the small penetration depth one would expect with such a high value of the loss factor. Since in the experiments in [4] there was no evidence of a strongly overheated surface of the reactant, the temperature was apparently homogenized by convection flows playing an apparently notable role here in the graphite-acid mixture as well.

These observations obtained from two different computational approaches to the same problem suggest that study of the effect of selective heating should continue toward further clarification of thermal processes in the reaction of technique [4].

Other aspects of the model that seem to be worth further improving include:

- Investigation of the scenarios with different EM fields in graphite and in the acids (due to their different complex permittivity).
- Incorporation of the effect of changing EM and T material parameters with temperature in the course of the chemical reaction.
- Consideration of heat release and absorption from the chemical reaction.

5 Conclusion

In this project, we have introduced, for the first time, three macroscopic models aiming to help clarify the features of thermal processes in the new technology of microwave-enabled production of solution-processable graphene sheets [4].

- The first model predicts microwave-induced temperature distribution in solid or high viscosity reactants by solving the fully coupled EM-T problem by the 3D conformal FDTD technique (using *QW-3D*).
- The second model is a simplified physics-based model studying the average temperature of liquid reactants in a three-media concentric cylindrical structure. The model is shown to provide highly accurate results (when the absorbed microwave power data is known) and takes negligible computational time.
- Finally, we have considered the effect of selective heating that seemingly takes place in the specific chemical reaction of production of graphene [4] by modeling temperature of two components of the reactant, graphite powder and the acids, separately. The preliminary results suggest the effect of selective heating of the powder mixed into H_2SO_4 and NHO_3 .

Overall, the results of this MQP have made an initial contribution to the development of a series of computational means assisting in further development (desirably, up to the industrial scale) of the new efficient technology of microwave-enable production of graphene.

Appendix

MATLAB Codes

A. Solving the System (18) & (19)

```
close all;
clear all;
clc;

dt = 3; %[s] time step in updating reflected power
Ploss = dlmread('RefPower2.txt');% a txt file that contains reflected power.
nt = size(Ploss, 1)-1; % extract time from .txt file

IC = zeros(2,1);
IC(1) = 21.4; % Initial temperature for medium 1
IC(2) = 21.4; % Initial temperature of medium 3

time = [1:dt:(nt+1)*dt]; % time

[tout, u] = ode45('usys2', time, IC); % Solve system of ODE

figure() % plot temperature of medium 1 and medium 3
hold on
plot(time-1,u(:,1),'*-'); % plot temperature of medium 1
plot(time-1,u(:,2),'o-');% plot temperature of medium 3
hold off
legend('medium 1', 'medium 3');
```

Function usys2.m

```
function du = usys2(t,u)
%modified 2/7/13 C Yang
%linear system for temperature of medium 1 and 3.
% u(1) - temperature of medium 1 (water)
% u(2) - temperature of medium 3 (Teflon)
% medium 2 - Pyrex

P = 100;%[W], Total incident power
Ploss = dlmread('RefPower2.txt');% file containing reflected power data
PlossAvg = mean(Ploss);% take average, given input data varies little.
alpha3= 0.124E-6;%[m^2/s] diffusivity of medium 3
alpha1 = 0.143E-6; %[m^2/s] diffusivity of medium 1
R = 1E-2; %[m], radius of medium 1
c1 = 4.18; %[J/(g*K)], 1J = 1W*s
m1 = 15.7; %[g] total mass of medium 1

a = 2E-3; %[m], thickness of medium 2
b = 2.25E-3; %[m], thickness of medium 3

D1 = 2*alpha1/R;
D3 = 2*alpha3*(R+a)/(2*b*(R+a)+b^2);
q = (P-PlossAvg)/(c1*m1);

du = zeros(size(u));

k2 = 1;% [W/(m*K)]thermal conductivity of medium 2
k1 = 0.6; % thermal conductivity of medium 1
k3 =0.25; % thermal conductivity of medium 3

du(1)= D1*k2/(a*k1)*u(2) - D1*k2/(a*k1)*u(1)+ q;
du(2) = -D3*k2/(a*k3)*u(2) + D3*k2/(a*k3)*u(1);

end
```

B. Finite Difference Solution to (22) and (23)

```
% numerically solve for graphite-acid model
clear all;
close all;
clc;

dt = 1000; % time step
dr = 1;
real_t = 30; %[s]actual reaction time

alpha1 = 3.6;% [mm^2/s] diffusivity of graphite
R = 20E-3; %[mm]radius of graphite
```



```

P = 100; % [W] total absorbed power

nt = round(real_t*alpha1/R^2/dt);

r1 = 10;%space step in graphite
r2 = 1000; %space step in acids

nr = r1+r2; %space step

alpha2 = 1.098E-1;%[mm^2/s] diffusivity of water

k1 = 6; %[w/(mk)]
k2 = 0.377; %[w/(mk)]
%

diag_alpha = [ones(1, r1), (alpha2/alpha1)*ones(1, r2)];
% non-d alpha with alpha_2/alpha1 ratio

alpha = diag(diag_alpha, 0); % matrix for diffusivity, alpha1... alpha2 on
diag.

%double space derivative matrix
Drr = diag(-2*ones(1, nr),0);
Drr = Drr + diag(ones(1, nr-1),1);
Drr = Drr + diag(ones(1, nr-1),-1);
Drr(1,:) =0; % insulated
Drr(end,:) = 0; % insulated on far end

%----- thermal BC between 2 media -----

Drr(r1, r1+1) = 0;
Drr(r1,r1) = -1;
Drr(r1+1,r1+2) = 0;
Drr(r1+1, r1) = 1+(k1+k2)/k2;
Drr(r1+1, r1-1) = -k1/k2;

%-----

A = eye(nr)/dt - alpha*Drr/(dr^2); % implicit differentiation
B = eye(nr)/dt;

%-----
% Thermal properties
c1 = 0.709; %[J/(g*K)] specific heat of graphite
c2 = 1.9; %[J/(g*K)] specific heat of water

m1 = 0.02; % [g] mass of graphite
m2 = 16.16; % [g] mass of water

eps1 = 27.47; %loss factor of graphite (data 10.5~14.5)
eps2 = 94.88; % loss factor of water,at ~ 25C.

```

```

V1 = 8.89E-3; % [cm^3] volume of graphite
V2 = 10; % [cm^3] volume of water

beta2 = eps2*V2/(eps1*V1 + eps2*V2);
beta1 = eps1*V1/(eps1*V1 + eps2*V2);

P1 = P*beta1;
P2 = P*beta2;

%-----
Phi1 = P1/(c1*m1);
Phi2 = P2/(c2*m2);
%
tilde_Phi = [Phi1*ones(1,r1), Phi2*ones(1,r2)]'; % dimensional heat source
term
%
Phi = R^2/alpha1.*tilde_Phi; % heat source terms

U = zeros(nr, nt+1);
U(:,1) = 0;

for i = 1:nt
U(:,i+1) = CN1(U(:,i), A, B, Phi);
end

T = U+20; % add room temp 20C.

r_real = linspace(0,R*(r1+r2)/r1,nr)*10^3;% dimensional r

t_real_v = linspace(0,real_t, nt);

figure()
hold on
plot(r_real, T(:,1), ':');
plot(r_real, T(:,round((nt+1)/4)), '-. ');
plot(r_real, T(:,round((nt+1)/2)), '-- ');
plot(r_real, T(:,round(3*(nt+1)/4)), '-- ');
plot(r_real, T(:,end), '- ');
hold off
legend('t=0', 't = 7.5s', 't = 15s', 't = 22.5', 't = 30s')
xlabel('distance from center [\mu m]')
ylabel('Temperature [C]')

```

Function CN1 .m

```
function [ U ] = CN1( S, A, B, Phi )
%S - Temp of previous iteration
%U - Temp of current iteration

U = A \ (B*S+Phi);

end
```

References

- [1] C.O. Kappe and A. Stadler, *Practical Microwave Synthesis for Organic Chemists: Strategies, Instruments, and Protocols*, Wiley-VCH, 2009.
- [2] N.E. Leadbeater, *Microwave Heating as a Tool for Sustainable Chemistry*, CRC Press, 2010.
- [3] A.O. Holmes, C. Yang, and V.V. Yakovlev, Temperature modeling for reaction development in microwave-assisted chemistry, In: *IEEE MTT-S Intern. Microwave Symp. Dig., Seattle, WA, June 2013* (to be published).
- [4] P.L. Chiu, D.D.T. Mastrogiovanni, D. Wei, C. Louis, M. Jeong, G. Yu., P. Saad, C.R. Flach, R. Mendelsohn, E. Garfunkel, and H. He, Microwave- and nitronium ion-enabled rapid and direct production of highly conductive low-oxygen graphene, *J. Am. Chem. Soc.*, vol. 134, pp. 5850-5856, 2012.
- [5] P. Kopyt and M. Celuch, Modeling microwave heating in foods, In: *Development of Packaging and Products for Use in Microwave Ovens*, M.W. Lorence and P.S. Pesheck, Eds., Woodhead Publishing, 2009, pp. 250-294.

- [6] T.V. Koutchma, and V.V. Yakovlev, Computer modeling of microwave heating processes for food preservation, In: *Mathematical Analysis of Food Processing*, M.M. Farid, Ed., CRC Press, 2010, pp. 625-657.
- [7] S.M. Allan, M.L. Fall, E.M. Kiley, P. Kopyt, H.S. Shulman, and V.V. Yakovlev, Modeling of hybrid (heat radiation and microwave) high temperature processing of limestone, In: *IEEE MTT-S Intern. Microwave Symp. Dig., Montreal, Canada, June 2012*, 978-1-4673-1088-9/12, pp. 1-4, 2012.
- [8] J. Subbiah, J. Chen, K. Pitchai, S. Birla, and D. Jones, Simulation of microwave heating of porous media coupled with heat, mass and momentum transfer in food product in domestic microwave oven using *COMSOL Multiphysics*, In: *COMSOL Conference Boston, MA, October 2012*.
- [9] E.K. Murphy and V.V. Yakovlev, CAD technique for microwave chemistry reactors with energy efficiency optimized for different reactants, *ACES J.*, vol. 25, pp. 1108-1117, 2010.
- [10] *QuickWave-3D™*, QWED Sp. z o. o., <http://www.qwed.com.pl/>
- [11] W.M. Haynes, *Handbook of Chemistry and Physics*, 93rd Ed., CRC Press, 2012.
- [12] R.C. Zeller, and R.O. Pohl, R.O., Thermal conductivity and specific heat of noncrystalline solids, *Phys. Rev. B*, vol. 4, pp. 2029-2041, 1971.
- [13] Teflon PTFE Properties Handbook, http://www.rjchase.com/ptfe_handbook.pdf , 1996.
- [14] P. Lidstrom, J. Tierney, B. Wathey, and J. Westman, Microwave assisted organic synthesis – a review, *Tetrahedron*, vol. 57, pp. 9225-9283, 2001.
- [15] H. He, Personal communications, 2012-2013.
- [16] J.M. Catalá-Civera, Personal communications, 2013.